ARTICLE
Journal of Cellular Biochemistry 113:80–92 (2012)

Journal of Cellular Biochemistry

LPS Induces Phosphorylation of Actin-Regulatory Proteins Leading to Actin Reassembly and Macrophage Motility

Galyna Kleveta,[1,2] Kinga Borzęcka,[1] Mykola Zdioruk,[1,2] Maciej Czerkies,[1] Hanna Kuberczyk,[1] Natalia Sybirna,[2] Andrzej Sobota,[1] and Katarzyna Kwiatkowska[1*]

[1]*Department of Cell Biology, Nencki Institute of Experimental Biology, 3 Pasteur St., 02-093 Warsaw, Poland*

[2]*Department of Biochemistry, Ivan Franko Lviv National University, 4 Hrushevsky St., 79005 Lviv, Ukraine*

ABSTRACT

Upon bacterial infection lipopolysaccharide (LPS) induces migration of monocytes/macrophages to the invaded region and production of pro-inflammatory mediators. We examined mechanisms of LPS-stimulated motility and found that LPS at 100 ng/ml induced rapid elongation and ruffling of macrophage-like J774 cells. A wound-healing assay revealed that LPS also activated directed cell movement that was followed by TNF-α production. The CD14 and TLR4 receptors of LPS translocated to the leading lamella of polarized cells, where they transiently colocalized triggering local accumulation of actin filaments and phosphatidylinositol 4,5-bisphosphate. Fractionation of Triton X-100 cell lysates revealed that LPS induced polymerization of cytoskeletal actin filaments by 50%, which coincided with the peak of cell motility. This microfilament population appeared at the expense of short filaments composing the plasma membrane skeleton of unstimulated cells and actin monomers consisting prior to the LPS stimulation about 60% of cellular actin. Simultaneously with actin polymerization, LPS stimulated phosphorylation of two actin-regulatory proteins, paxillin on tyrosine 118 by 80% and N-WASP on serine 484/485 by 20%, and these events preceded activation of NF-κB. LPS-induced protein phosphorylation and reorganization of the actin cytoskeleton were inhibited by PP2, a drug affecting activity of tyrosine kinases of the Src family. The data indicate that paxillin and N-WASP are involved in the reorganization of actin cytoskeleton driving motility of LPS-stimulated cells. Disturbances of actin organization induced by cytochalasin D did not inhibit TNF-α production suggesting that LPS-induced cell motility is not required for TNF-α release. J. Cell. Biochem. 113: 80–92, 2012.

KEY WORDS: ACTIN CYTOSKELETON; CELL MOTILITY; LPS; N-WASP; PAXILLIN; SRC KINASES

Lipopolysaccharide (LPS) is a component of the outer membrane of Gram-negative bacteria, which upon infection strongly activates neutrophils, monocytes, and macrophages. Activation of these cells requires a cascade of events starting from an interaction of LPS with LPS-binding protein in the serum. This protein delivers LPS to CD14, a GPI-anchored protein of the leukocyte plasma membrane. Subsequently, CD14 transfers LPS to a receptor complex comprising a transmembrane receptor, TLR4, and an extracellular protein MD2. LPS binds to a hydrophobic pocket of MD2 and directly mediates dimerization of two TLR4–MD2 complexes [Park et al., 2009]. TLR4 dimerization is believed to trigger signaling pathways leading, among others, to migration of leukocytes to the site of the infection and to production of pro-inflammatory cytokines like TNF-α and type I interferons [Poltorak et al., 1998; Kawai et al., 2001; Kagan and Medzhitov, 2006; Kagan et al., 2008; Tajima et al., 2008].

If excessive host responses to LPS take place, a systemic inflammatory condition named sepsis develops, which can lead to multiple organ failure and fatal septic shock. During these processes LPS-stimulated monocytes/macrophages and neutrophils migrate from blood vessels and accumulate in tissues producing high amounts of damaging pro-inflammatory mediators. Therefore, inhibition of leukocyte motility can provide means to limit the inflammatory reactions toward LPS. Accordingly, it was found that reduced neutrophil migration into liver and renal decreased by 80% the mortality of mice evoked by injection of high doses of LPS

Abbreviations used: PD buffer, HEPES-buffered saline; PHEM buffer, Pipes-HEPES buffer; PI(4,5)P_2, phosphatidylinositol 4,5-bisphosphate; PLC-PH-GST, pleckstrin homology domain of phospholipase $C_{\delta 1}$ and GST tag; PP2, 4-amino-5-(4-chlorophenyl)-7-(*t*-butyl)pyrazolol[3,4-*d*]pyrimidine.

Grant sponsor: National Science Center; Grant number: N N301 555240; Grant sponsor: Jozef Mianowski Found.

*Correspondence to: Katarzyna Kwiatkowska, Department of Cell Biology, Nencki Institute of Experimental Biology, 3 Pasteur St., 02-093 Warsaw, Poland. E-mail: k.kwiatkowska@nencki.gov.pl

Received 12 August 2011; Accepted 17 August 2011 • DOI 10.1002/jcb.23330 • © 2011 Wiley Periodicals, Inc.
Published online 24 August 2011 in Wiley Online Library (wileyonlinelibrary.com).

[Lowell and Berton, 1988]. This was achieved by double knockout of *hck* and *fgr* genes encoding two protein tyrosine kinases of the Src family, pointing to these kinases as crucial regulators of LPS-induced neutrophil motility. Those authors suggested that the defects in migration of Hck/Fgr-deficient neutrophils were due to disturbances in the signaling leading to actin cytoskeleton rearrangements [Lowell and Berton, 1988]. Indeed, further studies demonstrated that the kinases regulate migration of macrophages and neutrophils by affecting the interplay between Rac and Rho GTPases [Continolo et al., 2005; Fumagalli et al., 2007].

Studies on the motility of cultured vertebrate cells like fibroblasts have revealed that the process relies on the protrusion of the leading edge of the cell, its adhesion to the underlying substratum, retraction of the rear and de-adhesion [Pollard and Borisy, 2003]. The advancing of the leading edge is driven by polymerization of actin under the plasma membrane which supports extension of the plasma membrane in the form of lamellipodia and filopodia. Actin polymerization is accelerated mainly by de novo nucleation of fast growing barbed ends of actin filaments with the help of the Arp2/3 complex and its activators including WASP, N-WASP, and Scar/WAVE proteins. Activity of these proteins is, in turn, regulated by multiple factors including the Rho family GTPases Rac1 and Cdc42, phosphatidylinositol 4,5-bisphosphate ($PI(4,5)P_2$), and serine and tyrosine phosphorylation [Machesky and Insall, 1998; Nakagawa et al., 2001; Wu et al., 2004; Tomasevic et al., 2007]. Protrusion of the cell front is correlated with establishing new adhesion foci with extracellular matrix mediated by transmembrane integrins which tether actin filaments to the plasma membrane via an elaborate complex of proteins with paxillin, an adaptor protein phosphorylated at multiple tyrosine and serine residues, being among the first ones to localize to these sites [Laukaitis et al., 2001]. A recent mass spectrometric analysis has revealed that cytoskeletal proteins are among the "hot spots" of phosphorylation in LPS-stimulated macrophages [Weintz et al., 2010].

In the present study, we found that LPS activates migration of J774 macrophage-like cells followed by TNF-α production. Motility of cells was correlated with translocation of TLR4 and CD14 to the leading edge of the cells, transient phosphorylation of paxillin on Tyr118 and N-WASP on Ser484/485 and polymerization of cytoskeletal actin filaments. Disturbances of actin organization induced by cytochalasin D did not inhibit TNF-α production suggesting that LPS-induced cell motility is not required for TNF-α release.

MATERIALS AND METHODS

CELL CULTURE AND ACTIVATION

J774A.1 macrophage-like cells were cultured in DMEM supplemented with 10% FCS at 5% CO_2 (37°C). Cells were stimulated at 37°C with 100 ng/ml LPS prepared in the medium collected from the cultures and sonicated prior to use. Ultra pure LPS from *Escherichia coli* 0111;B4 was obtained from List Biological Laboratories (CA). When indicated, cells were preincubated for 30 min at 37°C with 10 μM 4-amino-5-(4-chlorophenyl)-7-(*t*-butyl)pyrazolol[3,4-*d*]pyrimidine (PP2, Calbiochem, CA) or with 5 μM cytochalasin D (Sigma, Poznan, Poland) or with 0.05–0.1% DMSO as a drug carrier; the drugs were also present during stimulation of cells with LPS. Experiments applying cytochalasin D were conducted in DMEM containing 1% FCS.

WOUND-HEALING ASSAY

Cells were seeded at 1.2×10^6 in 30-mm Petri dishes and grown to 90% confluence for 24 h. Cell monolayers were wounded with sterile micropipette tips forming a uniform in width cell-free zone. After washing with PBS, the cultures were supplemented with DMEM/0.5% FCS with or without 100 ng/ml LPS. Cells were monitored and photographed with a Nikon Eclipse TS100 inverted microscope equipped with a DXM 1200 C digital camera. Artificial lines fitting the cutting edges were drawn on pictures of the selected wounds which were captured within 15 min after formation and overlaid on the pictures of cultures taken in the course of incubation with or without 100 ng/ml LPS. Cell migrating to the cell-free area were counted in three randomly selected fields in three experiments.

FRACTIONATION OF ACTIN CYTOSKELETON

For experiments, cells (0.5×10^6/well in 24-well plates) were transferred into DMEM containing 1% FCS for 18 h. At different time-points of LPS stimulation cells were washed with PD buffer (125 mM NaCl, 4 mM KCl, 10 mM $NaHCO_3$, 1 mM KH_2PO_4, 10 mM glucose, 1 mM $CaCl_2$, 1 mM $MgCl_2$, 20 mM HEPES, pH 7.4) and lysed in 200 μl of a buffer composed of 0.5% Triton X-100, 100 mM KCl, 5 mM $MgCl_2$, 2 mM EGTA, 25 mM Tris, pH 7.5 and a protease inhibitor cocktail. After 10 min (4°C), cell lysates were fractionated according to Hartwig and Shevlin [1986] and Fox et al. [1988] with modifications, as follows. Material solubilized in 0.5% Triton X-100 was collected for further fractionation while the cytoskeleton attached to the substratum was washed once in the buffer containing 0.5% Triton X-100, dissolved in 200 μl of 8 M urea, 7 mM $CaCl_2$, 2 mM ATP, supplemented with SDS–PAGE sample buffer and boiled (cytoskeletal actin). The collected supernatants were centrifuged for 10 min at 10,000*g* to pellet cellular debris which were discarded. After withdrawing 10 μl-samples for SDS–PAGE analysis, the supernatants were subjected to high-speed centrifugation (1 h, 100,000*g*) to separate actin monomers (supernatant) and plasma membrane skeleton (pellet). The pellet was dissolved in 30 μl of the urea solution and analyzed by SDS–PAGE. To quantify actin in isolated fractions, equal volume of each fraction was applied onto a gel. After immunoblotting with anti-actin antibody, actin bands were analyzed densitometrically using ImageJ software (NIH, MD). Actin content in each fraction at different stages of LPS stimulation was expressed as a percentage of actin amount found in unstimulated cells in the corresponding set of fractions.

IMMUNOFLUORESCENCE STUDIES

Cells (2.5×10^5/coverslip) were stimulated with LPS, washed with ice-cold PD buffer and transferred onto ice. Cells were next incubated with 10% mouse serum (Jackson ImmunoResearch, PA) and exposed to rabbit anti-TLR4 (Santa Cruz Biotechnology, CA) in the presence of 5% mouse serum, followed by sheep anti-rabbit IgG-biotin (Rockland Immunochemicals, PA) (4°C, 30 min each incubation in DMEM/5% FCS and 20 mM HEPES, pH 7.4). Cells were fixed with 4% formaldehyde in PHEM buffer (60 mM Pipes, 25 mM

HEPES, 10 mM EGTA, 4 mM $MgCl_2$, pH 6.9), exposed to 50 mM NH_4Cl/PHEM (5 min, 25°C) and 3% BSA in TBS (30 min, 25°C). The samples were incubated with rat anti-CD14 antibody (Santa Cruz Biotechnology) and next with donkey anti-rat IgG-Texas Red (Jackson ImmunoResearch) and ExtrAvidin-FITC (Sigma) (each incubation 30 min, 25°C in TBS containing 0.2% BSA) to visualize CD14 and TLR4 on the cell surface, respectively. When indicated, cells were permeabilized with 0.005% digitonin/PHEM (10 min, 25°C), blocked with 3% BSA/PHEM (30 min, 25°C) and incubated with following probes: phallodin-TRITC (Sigma), phalloidin-Alexa Fluor 350 (Invitrogen, CA), 1 μg/ml of a fusion protein containing the pleckstrin homology domain of phospholipase $C_{\delta 1}$ and GST tag (PLC-PH-GST, a specific marker of $PI(4,5)P_2$) or 1 μg/ml GST as a control [Szymanska et al., 2009]. The two probes were visualized with goat anti-GST (Rockland Immunochemicals) and donkey anti-goat IgG-Texas Red (Jackson ImmunoResearch). Each incubation was conducted for 60 min at 25°C in TBS/0.2% BSA. In a series of experiments, cell surface labeling of proteins was omitted. After fixation, permeabilization and blocking, cells were incubated with rabbit IgG anti-phospho-paxillin (Tyr118; Cell Signaling, MA) or rabbit IgG anti-phospho-N-WASP (Ser484/Ser485; Imgenex, CA) followed by goat anti-rabbit IgG $F(ab)_2$-FITC (Jackson ImmunoResearch) and phalloidin-TRITC. In the course of these procedures all solutions were supplemented with 50 μM phenylarsine oxide and 1 mM Na_3VO_4. In control samples, when primary antibodies were omitted, negligible immunofluorescence was found. Samples were mounted in mowiol/DABCO and examined under a Leica confocal microscope with sequential excitation of FITC and Texas Red or TRITC to avoid crossover of their fluorescence. Colocalization of TLR4 and CD14 was analyzed using Leica Application Suite AF software which calculated Pearson's correlation coefficient and overlap coefficient essentially as described earlier [Kulma et al., 2010]. At least 40 cells from two independent experiments were analyzed for each variant.

MORPHOMETRIC ANALYSIS

Cells were cultured on coverslips, transferred to DMEM/1% FCS for 18 h, stimulated with LPS and labeled with phalloidin-TRITC according to the protocol described above. Samples were viewed under a Nikon microscope equipped with a DXM 1200 C digital camera. The number of cells with ruffles was counted and the cell length was measured on the collected images using ImageJ software. The calculations were performed in three independent experiments from 10 to 15 fields containing a total of 100 to 150 cells for each sample.

TNF-α AND RANTES ASSAYS

Cells (0.5×10^5/well in 96-well plates) were stimulated with 100 ng/ml LPS for 4 h at 37°C and TNF-α and RANTES levels in culture supernatants were determined with the use of murine ELISA kits (BioLegend, CA; R&D, MN) according to the manufacturer's instructions, using a Sunrise plate reader (Tecan Group, Mannedof, Switzerland). When cytochalasin D was applied, cells were incubated with 5 μM drug (or an equivalent amount of DMSO) for 30 min at 37°C in DMEM/1% FCS and stimulated with LPS for 4 h in the presence of cytochalasin D diluted to final concentration of 1 μM in DMEM/1% FCS.

IMMUNOBLOTTING

Cells (1.5×10^5) were lysed in 50 μl of buffer containing 0.5% Triton X-100, 100 mM NaCl, 2 mM EGTA, 2 mM EDTA, 20 mM HEPES, pH 7.4, 50 μM phenylarsine oxide, 20 mM *p*-nitrophenylphosphate, 1 mM Na_3VO_4, and a cocktail of protease inhibitors (10 min, 4°C) and supplemented with SDS–PAGE sample buffer. The lysates as well as cellular fractions were subjected to SDS–PAGE, transferred onto nitrocellulose sheets and immunoblotted essentially as described [Kwiatkowska et al., 2003]. The following antibodies were used: rabbit IgG anti-phospho-paxillin (Tyr118), mouse IgG anti-phospho-IκB (Ser32/35) (both Cell Signaling, MA) and rabbit IgG anti-phospho-N-WASP (Ser484/Ser485; Imgenex). The primary antibodies were followed by either anti-mouse or anti-rabbit IgG conjugated with peroxidase (Jackson ImmunoResearch, Rockland Immunochemicals). To verify equal loading of proteins in samples, the membranes were stripped and reprobed with mouse IgG anti-actin antibody (MP Biomedicals, OH) followed by anti-mouse IgG-peroxidase. The immunoreactive bands visualized by chemiluminescence (Pierce, IL) were analyzed densitometrically using the ImageJ software. Signals corresponding to the phospho-proteins were normalized against actin content in the sample. In a series of experiments, proteins transferred onto nitrocellulose were subjected to dephosphorylation with calf intestine phosphatase (Sigma; 5 U/ml, 60 min, room temperature) prior to incubation with anti-phospho-paxillin or anti-phospho-N-WASP antibody. After this procedure, no phospho-proteins were detected by the two antibodies.

DATA ANALYSIS

The significance of differences between groups was calculated using a Student's *t*-test. $P < 0.05$ was considered to be statistically significant.

RESULTS

LPS INDUCES MIGRATION OF J774 CELLS

In order to reveal how LPS activates motility of J774 cells, we examined the organization of the actin cytoskeleton in the course of 100 ng/ml LPS action. Prior to stimulation, cells were mostly rounded with actin filaments forming a cortical ring (Fig. 1A). When exposed to LPS, the cells polarized and elongated often displaying distinct lamellae with actin-rich ruffles at the leading edge, features typical of motile cells (Fig. 1B, arrows). The length of LPS-treated cells increased 1.5-fold after 20 min and remained at this level for up to 1 h (Fig. 1C,D). At 10–20 min of LPS action, the proportion of cells with ruffles doubled, and then within ca. 40 min decreased back to the level found in resting cells (Fig. 1D).

The effect of LPS on migration of J774 cells was further examined using a wound-healing assay. At the presence of 100 ng/ml LPS cells facing the wounded area polarized quickly. Their motility, reflected by number of cells entering the denuded zone, was escalated for up to 4 h in comparison to control cells (Fig. 1E,F). Later on, migration activity of LPS-treated cells progressively decelerated to that of

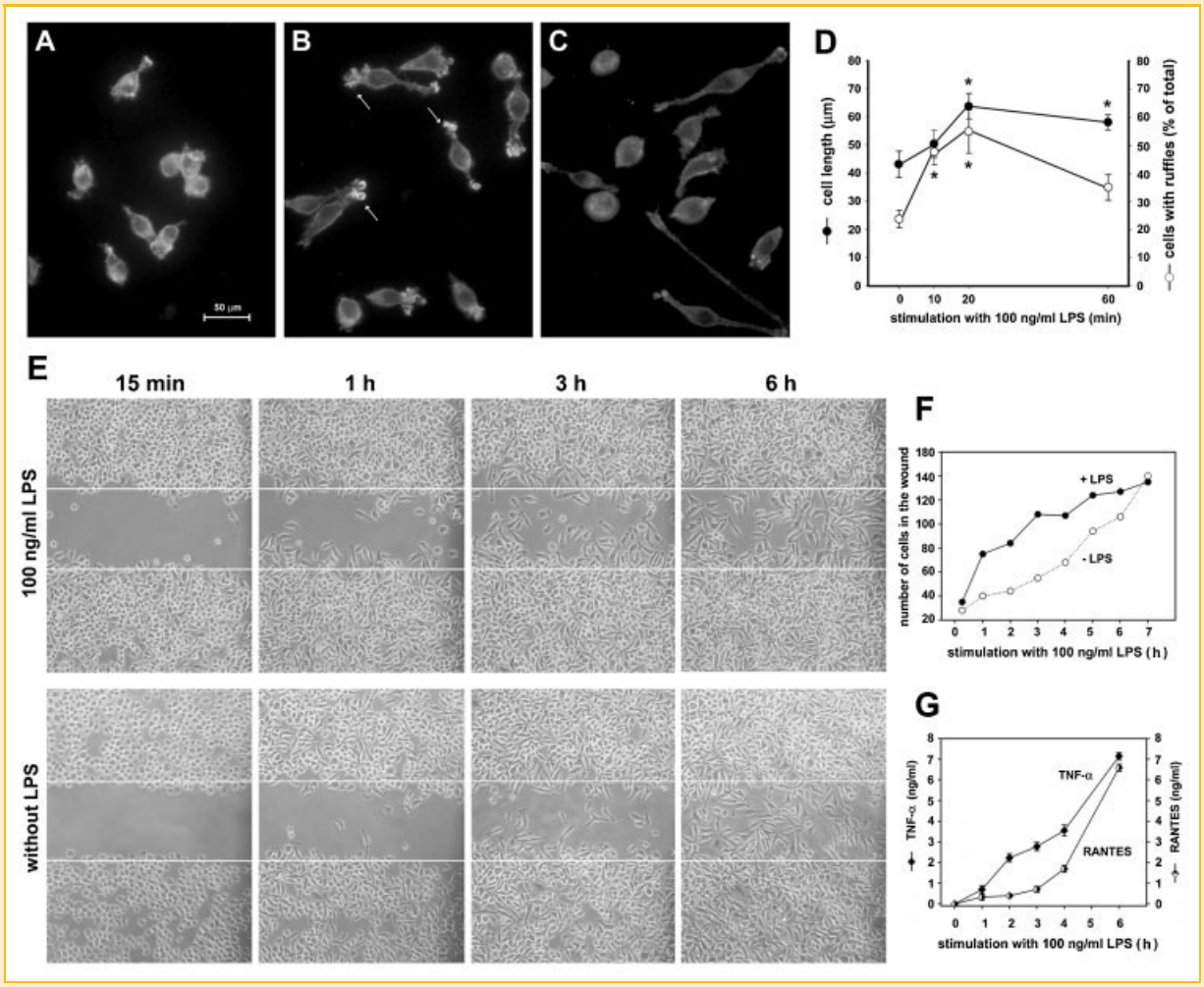

Fig. 1. LPS activates motility of J774 cells. A–C: Cells were left unstimulated (A) or exposed to 100 ng/ml LPS for 20 min (B) or 60 min (C), fixed, permeabilized, and labeled with phalloidin–TRITC to visualize actin filaments. Arrows indicate ruffles formed at the front of cells. D: Changes of cell length and number of cells exhibiting ruffling during stimulation with 100 ng/ml LPS. Data are mean ± SEM from three experiments. *Significantly different from unstimulated cells at $P < 0.05$. E: Migration of J774 cells determined in a wound-healing assay in the presence of 100 ng/ml LPS (upper panel) and the absence of LPS (lower panel). F: Number of cells entering cell-free zones demarcated in (E) in the course of stimulation with 100 ng/ml LPS (closed symbols) and without LPS (open symbols). E,F: Results from a pair of "wounds" representative to three examined fields in one of three independent experiments. G: Time course of TNF-α (filled symbols) and RANTES (semi-filled symbols) production by J774 cells stimulated with 100 ng/ml LPS. Data are mean ± SEM from three experiments run in triplicates.

unstimulated cells. The retardation of the movement of LPS-stimulated cells was correlated with a marked increase of production of TNF-α and RANTES cytokines by the cells (Fig. 1G).

The polarization of the LPS-stimulated cells was correlated with redistribution of the TLR4 and CD14 receptors in the plane of the plasma membrane. Both types of receptors accumulated at the leading edge of the polarized cells (Fig. $2A_1$–A_3, arrows). Small numbers of the receptors could be occasionally observed also at the trailing edge of polarized cells (Fig. $2A_1$–A_3, arrowhead). Colocalization of TLR4 and CD14 was studied on enlarged optical sections through the ventral and middle part of the lamella (Figs. $2B_1$–B_3,$2C_1$–C_3, respectively). Among two parameters which describe the colocalization, Pearson's correlation and overlap coefficients, the former was in the range of 0.5 with 1 as the maximal value. The Pearson's correlation coefficient provides information about the similarity of shape between two images without regard to the average intensity of the signals [Manders et al., 1993], and its value indicated marked colocalization of TLR4 and CD14 in lamellae of stimulated cells. The overlap coefficient reached even higher values (around 0.6), however, this parameter is affected by differences in the fluorescence patterns [Manders et al., 1993], like an excess CD14 over TLR4, between the compared images. The two LPS receptors remaining on the surface of the cell body behind the lamella did not colocalize (Fig. $2D_1$–D_3), as reflected by low values of the Pearson's correlation and overlap coefficients (below 0.3). TLR4 and CD14 were also separated, being randomly distributed, on the surface of cells prior to LPS stimulation (Fig. $2E_1$–E_3). This was reflected by values of the Pearson's correlation coefficient in the range of 0.25–0.35 and those of the overlap coefficient up to 0.5, as estimated at the ventral, middle, and dorsal optical sections of unstimulated cells (Fig. $2F_1$–H_3).

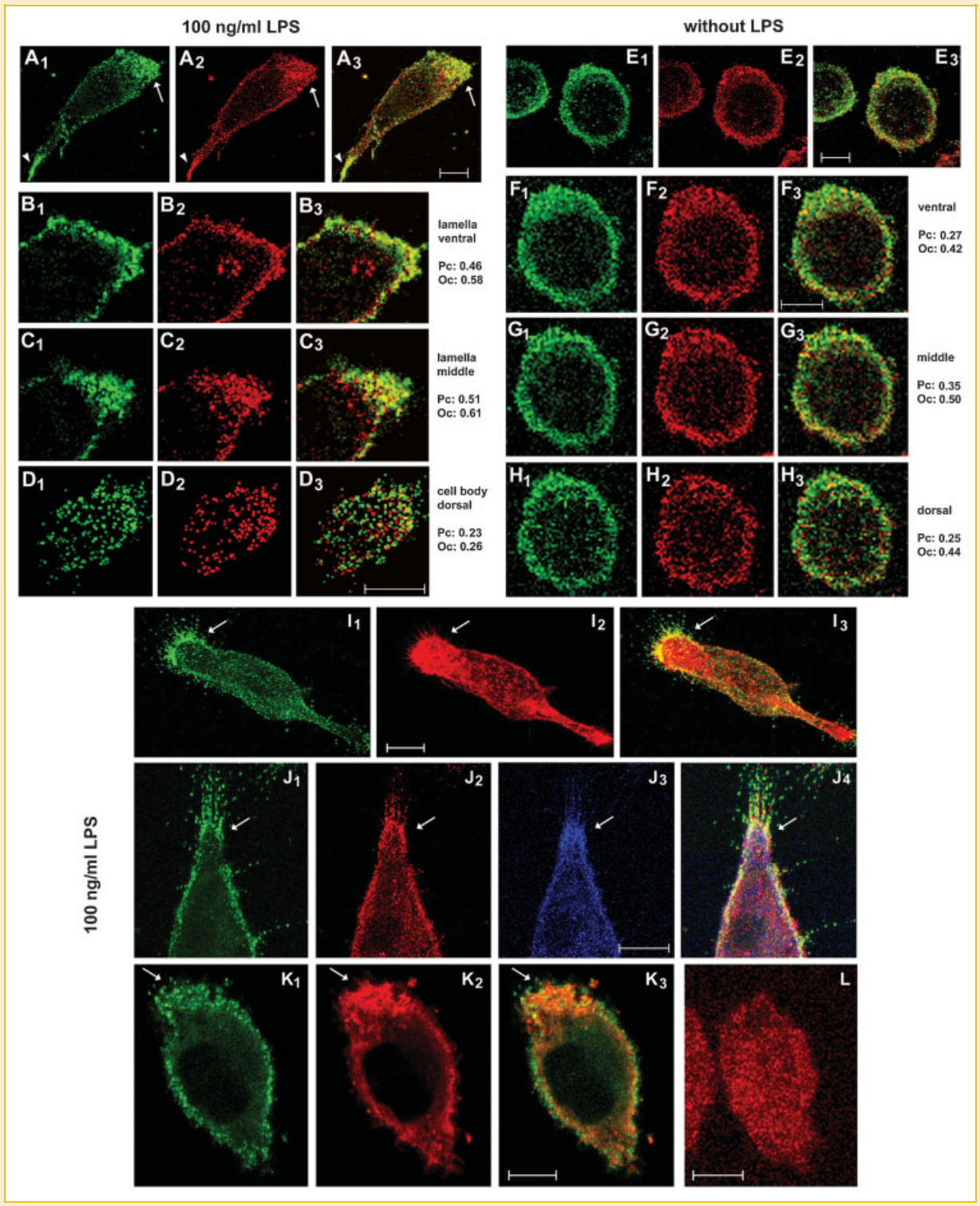

Fig. 2. TLR4 and CD14 colocalize at the leading lamella of LPS-stimulated cells. A_1–H_3: Cell surface distribution of TLR4 (green), CD14 (red), and merged images showing colocalization of the two receptors in the lamellae of LPS-stimulated and in resting cells. A_1–D_3: Cells stimulated with 100 ng/ml LPS for 20 min. B_1–D_3: Enlarged images showing single optical sections through ventral (B_1–B_3) and middle part of the lamella (C_1–C_3) and a dorsal optical section of the cell body behind the lamella (D_1–D_3). For better visualization of the proteins, the intensity of (D_1–D_3) was increased relative to (B_1–C_3). In (A_1–A_3) arrows indicate the leading lamella while arrowheads—the trailing edge of the cells. E_1–H_3: Unstimulated J774 cells. F_1–H_3: are enlarged optical sections through a cell from (E) taken at the ventral, middle, and dorsal part of the cells, as indicated. Values of Pearson's correlation (Pc) and overlap coefficient (Oc) were estimated for the optical sections shown and are representative for data obtained from at least 40 cells. I_1–L: Actin filaments and $PI(4,5)P_2$ accompany TLR4 and CD14 at the leading edge of LPS-stimulated cells. Cells were exposed to 100 ng/ml LPS for 20 min and labeled to visualize TLR4 (I_1,J_1,K_1, green) and CD14 (J_2, red) on the cell surface. After permeabilization, cells were exposed to phalloidin-TRITC (I_2, red) or phalloidin-Alexa Fluor 350 (J_3, blue), both staining actin filaments. To localize $PI(4,5)P_2$ cells were treated with PLC-PH-GST followed by goat anti-GST and anti-goat-Texas Red (K_2, red). (I_3, J_4, and K_3) show colocalization of the two or three fluorochromes analyzed. Arrows point to the leading edge of cells. L: A faint fluorescence found in control cells exposed to GST instead of PLC-PH-GST. Bars, 10 μm.

After LPS simulation, at the leading edge of polarized cells, where TLR4 and CD14 accumulated, abundant actin filaments were also found; microfilaments delineated the plasma membrane and filled ruffles on the dorsal surface of the lamellae (Fig. $2I_1$–J_4). In addition, the leading edge was also heavily decorated with PLC-PH-GST probe indicating local accumulation of $PI(4,5)P_2$, a lipid controlling activity of several actin-binding proteins (Fig. $2K_1$–K_3). In contrast, a negligible fluorescence was seen in control cells exposed to GST instead of the PLC-PH-GST fusion protein (Fig. 2L).

CYTOSKELETAL ACTIN FILAMENTS POLYMERIZE IN LPS-STIMULATED CELLS

To analyze the LPS-induced actin reorganization, cells were lysed in Triton X-100 to separate cytoskeletal actin filaments, remaining attached to the substratum, from solubilized actin. As seen in Figure 3A, the latter was subsequently fractionated into actin monomers and short actin filaments of the plasma membrane skeleton by high-speed (100,000*g*) centrifugation [Hartwig and Shevlin, 1986; Fox et al., 1988]. We applied quantitative immunoblotting to estimate the proportion of actin forming (I) the cytoskeletal filaments, (II) the membrane skeleton filaments, and (III) existing as monomer in the cells. In resting cells, these three actin forms represented, respectively, $34.0 \pm 1.5\%$, $5.9 \pm 0.5\%$, and $60.1 \pm 1.9\%$ ($n = 3$). Thus, monomeric actin dominated over the polymerized one in a 6:4 ratio. LPS triggered assembly of cytoskeletal actin filaments; the fraction of actin composing this population of filaments raised sharply by over 50% at 20 min and declined after 40 min of LPS action (Fig. 3B,C, closed circles). The polymerization of cytoskeletal actin paralleled a depletion of actin remaining in the low speed supernatant (Fig. 3B,C, open circles). Further fractionation of the supernatant into the plasma membrane skeleton actin and monomeric actin demonstrated that filaments of the plasma membrane skeleton were most abundant in unstimulated cells (Fig. 3B,D). This fraction of actin filaments depolymerized in LPS-challenged cells (Fig. 3B). After 60 min of stimulation, the proportion of actin forming the plasma membrane skeleton was reduced by nearly 50% (Fig. 3D).

TRANSIENT PHOSPHORYLATION OF PAXILLIN Tyr118 AND N-WASP Ser484/485 INDUCED BY LPS

Polymerization of actin filaments and their interaction with the plasma membrane are mediated, among others, by N-WASP and paxillin. We found that both these proteins were activated in the course of the actin reorganization triggered by LPS, judging by phosphorylation of paxillin tyrosine residue 118 and N-WASP serine residues 484/485 (Fig. 4A,B). The antibody specific toward paxillin phosphorylated on Tyr118 recognized three bands which migrated on SDS–PAGE with molecular weights of around 60–70 kDa (Fig. 4A). A heterogeneous electrophoretic mobility of paxillin attributed to its various patterns of phosphorylation was already reported [Schaller and Schaefer, 2001]. The level of paxillin phosphorylation on Tyr118 was fairly low in unstimulated cells and increased transiently between 10 and 30 min of LPS action reaching 180% of the initial value (Fig. 4A,C, closed circles). N-WASP Ser484/485 phosphorylation was relatively high already in unstimulated cells and upon challenge with LPS increased by 20% (20 min after stimulation), followed by dephosphorylation to a level below that in resting cells (Fig. 4B,C, closed circles). The increase of the levels of phospho-paxillin and phospho-N-WASP preceded the phosphorylation of IκB on Ser32/35 (30–60 min) which reflected activation of the NF-κB transcription factor by LPS (Fig. 4B,C, closed circles).

We examined cellular localization of phospho-paxillin and phospho-N-WASP to investigate an involvement of these proteins in actin filament reorganization induced by LPS. In unstimulated cells, discrete spots of paxillin phosphorylated on Tyr118 were seen at the cell periphery clearly delineated by the cortical actin ring (Fig. $5A_1$–A_2). Upon LPS stimulation, phospho-paxillin was enriched and located in small focal assemblies some of which were concentrated at the leading edge of cells (Fig. $5B_1$–B_2, arrows). Others spots of the protein were distributed across the lamella and in the uropod (Fig. $5B_1$–B_2). At the leading edge assemblies of phospho-paxillin colocalized with the proximal part of actin bundles forming microspikes and filopodia (Fig. $5C_1$–C_2).

Phospho-N-WASP was distributed diffusely in the cytoplasm of unstimulated cells with a moderate enrichment under the plasma membrane; the protein was also seen in the nucleus (Fig. $5D_1$–D_2). After LPS stimulation, a fraction of phospho-N-WASP accumulated at the leading edge of polarized cells, however, in contrast to phospho-paxillin, this protein was seen in a fairly continuous band parallel to the cell front and was present in ruffles (Fig. $5E_1$, arrows, Fig. $5F_1$, double arrows). Localization of phospho-N-WASP coincided with a frontal layer of abundant microfilaments and with actin in ruffles (Fig. $5E_1$–F_2).

ACTIVITY OF THE Src KINASES IS REQUIRED FOR ACTIN CYTOSKELETON REARRANGEMENTS IN LPS-STIMULATED CELLS

The phosphorylation of studied proteins was sensitive to PP2, an inhibitor of Src family tyrosine kinases. PP2 abolished LPS-induced phosphorylation of paxillin on Tyr118 (Fig. 4A,C, open circles) in agreement with this tyrosine residue of paxillin being a substrate of Src kinase [Schaller and Schaefer, 2001; Brown and Turner, 2004]. However, under the influence of PP2 also the serine phosphorylation of N-WASP was significantly diminished indicating that the Src family tyrosine kinases control indirectly the N-WASP Ser484/485 phosphorylation. PP2 affected N-WASP phosphorylation in resting cells and caused a delay and a reduction of this phosphorylation in LPS-challenged cells (Fig. 4B,C, open circles). Similarly, the inhibitor reduced serine phosphorylation of IκB with the inhibition reaching 50% at 30 min and becoming even more pronounced at 60 min of LPS action (Fig. 4B,C, open circles).

The inhibitory effect of PP2 on the phosphorylation of the two actin-regulatory proteins was correlated with disturbances of actin filament organization in the cells, leading to a depletion of cytoskeletal actin filaments and an increased proportion of actin in the fraction of short filaments and monomers (Fig. 4D, compare lane 1 with 5 and 9 with 13). In the presence of PP2 LPS did not induce polymerization/depolymerization of the cytoskeletal actin filaments (Fig. 4D, compare lanes 2–4 and 6–8; Fig. 4E). As a consequence, PP2-treated cells contained increased amounts of actin monomers/short filaments in comparison to control, DMSO-treated cells, regardless of LPS stimulation (Fig. 4D, compare lanes 9–12 and 13–16).

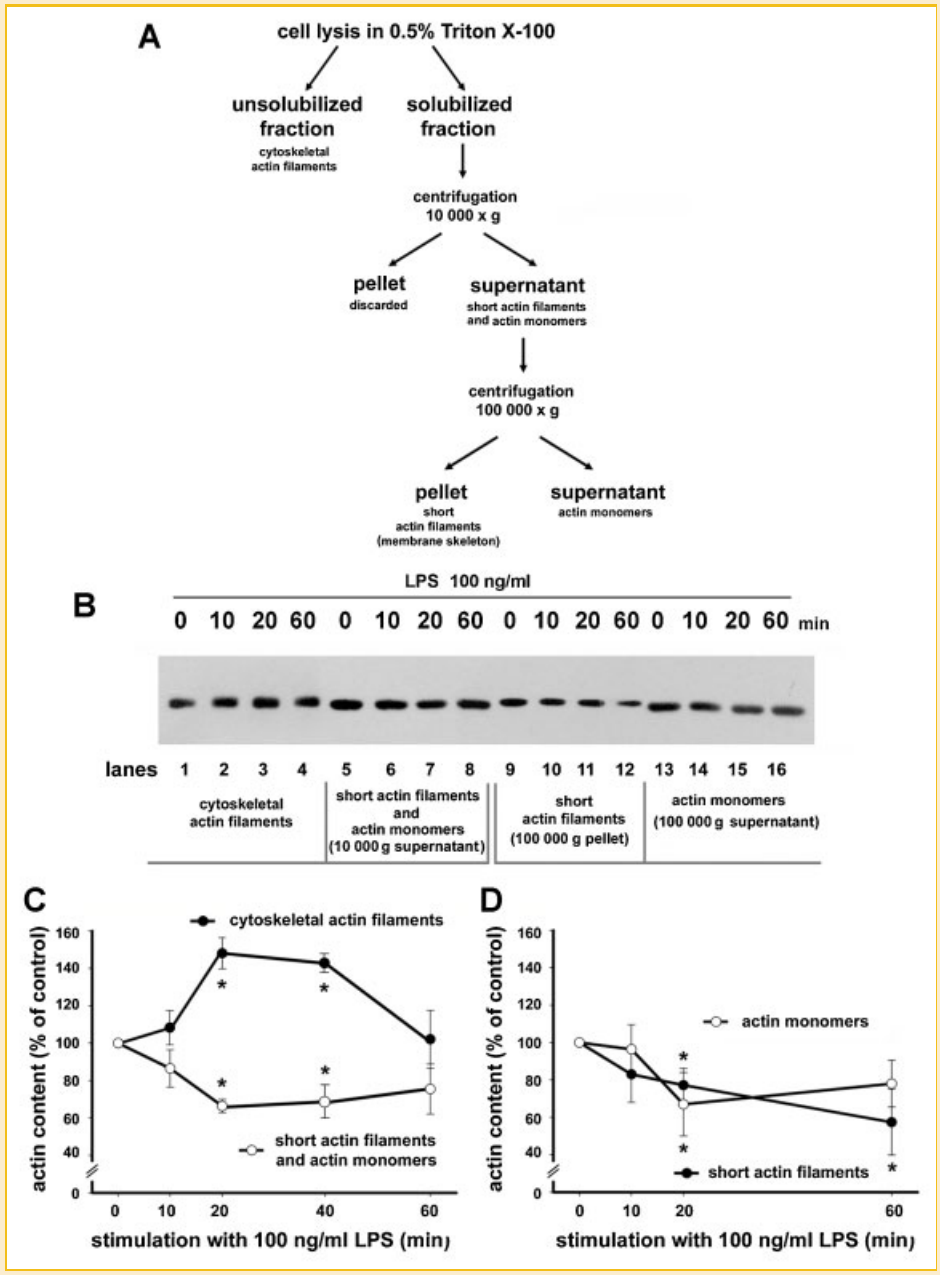

Fig. 3. LPS induces polymerization of cytoskeletal actin filaments and disassembly of plasma membrane skeleton. A: Scheme of fractionation of 0.5% Triton X-100 cell lysates into fractions containing cytoskeletal actin filaments, short actin filaments of the membrane skeleton, and actin monomers. B: Fractions from cells stimulated for 0–60 min with 100 ng/ml LPS and immunoblotted for actin. Equal volume of each fraction was applied onto the gel. C,D: Quantification of actin in fractions from cells stimulated with 100 ng/ml LPS, containing cytoskeletal filaments (C, closed circles), or a mixture of actin monomers and short actin filaments (C, open circles), the latter subsequently separated into short actin filaments (D, closed circles) and actin monomers (D, open circles). Analysis based on densitometry of immunoblots as in (B). Actin content in each fraction at different time-points of LPS stimulation was expressed as a percentage of actin amount found in unstimulated cells in the corresponding set of fractions. Data are the mean ± SEM from four or six experiments. *Significantly different from unstimulated cells at $P < 0.05$.

AN INFLUENCE OF ACTIN CYTOSKELETON DISTURBANCES ON LPS-TRIGGERED SIGNALING

As phospho-paxillin and phospho-N-WASP are likely to be engaged in the reorganization of actin filaments induced by LPS, we examined whether disturbances of actin skeleton affect reciprocally LPS-induced signaling. Under the influence of 5 μM cytochalasin D, an actin polymerization inhibitor, cells retracted from the substratum and underwent arborization forming numerous branched projections surrounding the body (Fig. 6A,B). In these condition, TLR4 and CD14 frequently gathered in joined clusters located around the cell body and in distal parts of plasma membrane projections (Fig. $6A_1$–A_3). The receptor clusters were likely to correspond to actin aggregates revealed by phalloidin-TRITC in cytochalasin D-treated cells (not shown). However, on the remaining

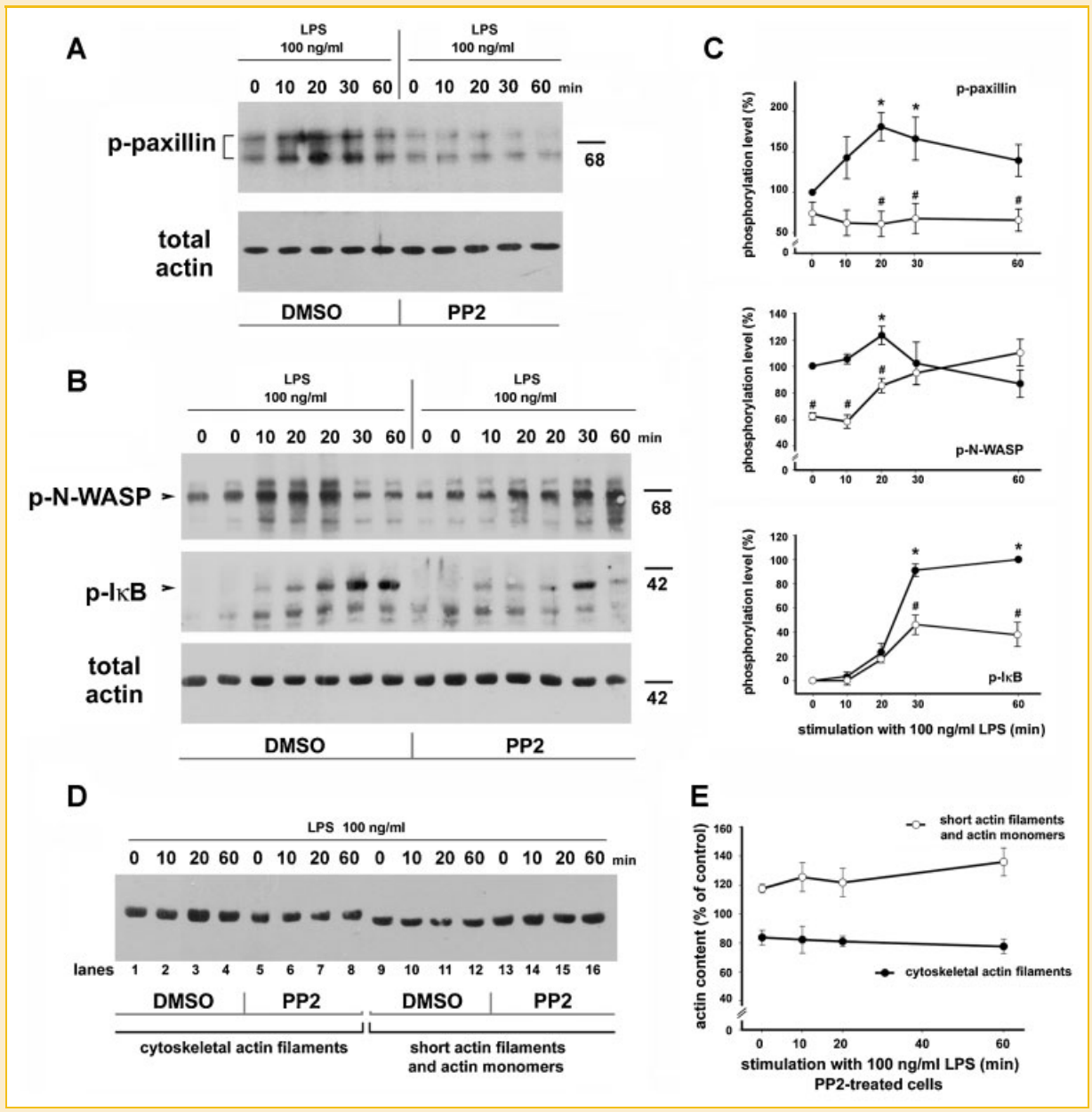

Fig. 4. LPS induces transient phosphorylation of paxillin and N-WASP that is inhibited by PP2. Cells were preincubated with PP2 or DMSO as a drug carrier and stimulated with 100 ng/ml LPS (0–60 min) in the presence of the two compounds. A: Whole cell lysates were probed with antibody specific toward paxillin phosphorylated on Tyr118 (p-paxillin). The same membrane was probed with anti-actin antibody to verify equal amounts of proteins loaded on the gel. B: Whole cell lysates probed for N-WASP phosphorylated on Ser484/Ser485 (p-N-WASP, upper part of the membrane) or IκB phosphorylated on Ser32/35 (p-IκB, lower part of the same membrane). After stripping, the membrane was labeled for actin to demonstrate equal loading of proteins. Positions of molecular weight markers: BSA of 68 kDa and actin of 42 kDa are shown on right. C: Phosphorylation levels of paxillin (top), N-WASP (middle), and IκB (bottom) during stimulation of cells with 100 ng/ml LPS based on densitometry of immunoblots as in (A,B). Data were normalized against actin level in samples and expressed as percentage of phospho-protein amount in unstimulated cells (paxillin and N-WASP) or as percentage of maximal phosphorylation found after 60 min of LPS action (IκB). Closed circles, control cells treated with DMSO; open circles, cells exposed to PP2. Data shown are mean ± SEM from four or five experiments. *Significantly different from unstimulated cells at $P < 0.05$, #significantly different at $P < 0.05$ form DMSO-treated cells at the corresponding time-point. D,E: Actin content in fractions of Triton X-100 lysates obtained from cells stimulated with 100 ng/ml LPS in the presence of PP2 or DMSO. D: Actin non-solubilized in Triton X-100 and remaining attached to substratum (cytoskeletal actin filaments) or solubilized in the detergent (short actin filaments and actin monomers). E: Densitometric quantification of actin in fractions from cells treated with PP2 and stimulated with 100 ng/ml LPS, containing cytoskeletal filaments (E, closed circles), or a mixture of actin monomers and short actin filaments (E, open circles). Actin content in each of two fractions expressed as a percentage of actin amount found in the corresponding fraction of unstimulated cells not treated with PP2. For the clarity, the volume of fractions loaded onto the gel presented in (D) containing short actin filaments/actin monomer was reduced by half in comparison to the volume of the cytoskeletal fraction samples. Data are the mean ± SEM from three experiments.

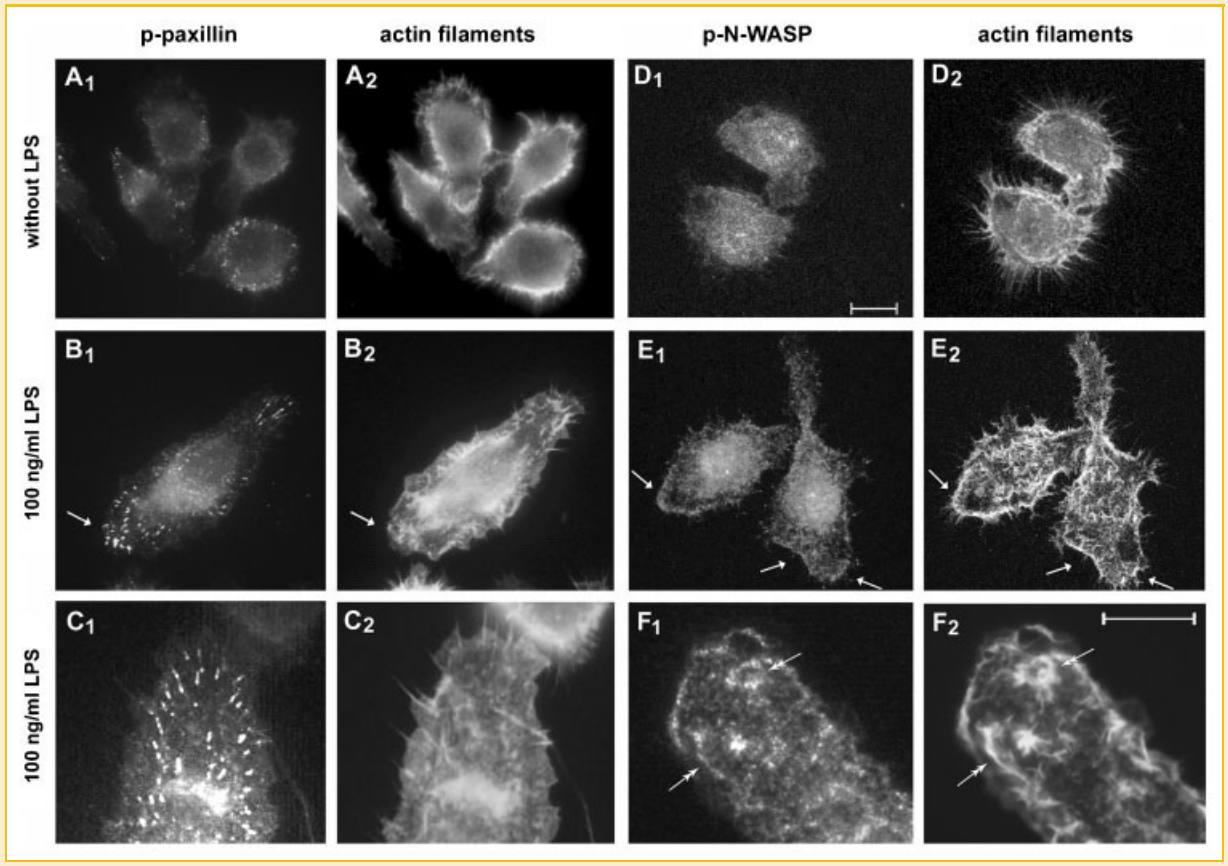

Fig. 5. Phospho-paxillin and phospho-N-WASP accumulate at the leading edge of LPS-stimulated cells. Localization of paxillin phosphorylated on Tyr118 (A_1,B_1,C_1) and N-WASP phosphorylated on Ser484/Ser485 (D_1,E_1,F_1) is shown in comparison to actin filaments (A_2–F_2). The upper panel shows cells prior to stimulation with LPS; in the middle and the lower panels cells exposed to 100 ng/ml LPS for 20 min are seen. The lower panel presents enlarged views of the leading lamellae of LPS-stimulated cells. Arrows in (B_1–B_2) and (E_1–E_2) point to accumulation of phospho-paxillin, phospho-N-WASP and actin filaments at the leading edge of stimulated cells. Double arrows in (F_1,F_2) indicate ruffles. Bars, 10 μm.

surface of thin projections of the plasma membrane the receptors were separated (Fig. 6A_1–A_3). As a result, the mean values of the Pearson's correlation and the overlap coefficients for TLR4 and CD14 were modest reaching 0.41 ± 0.014 and 0.46 ± 0.021, respectively. Treatment of cells with 100 ng/ml LPS (20 min) did not affect substantially either the pattern of TLR4 and CD14 distribution on the cell surface (Fig. 6B_1–B_3) or the colocalization rate of the two receptors (Pearson's correlation coefficient of 0.38 ± 0.026 and overlap coefficient of 0.43 ± 0.031).

Reorganization of actin filaments induced by cytochalasin D disturbed phosphorylation of paxillin on Tyr118 and N-WASP on Ser484/485. Under the influence of 5 μM cytochalasin D phosphorylation of the two proteins in unstimulated cells was observed and the process was not sensitive to 100 ng/ml LPS action (Fig. 6C,D). These data suggest that although tyrosine phosphorylation of actin-binding proteins, dependent on the Src kinases, controls reorganization of the actin cytoskeleton (see Fig. 4), the cytoskeleton may affect the protein phosphorylation in a feedback manner. Despite the disturbances of the actin cytoskeleton organization induced by cytochalasin D, no inhibition of TNF-α production was found after challenging cells with 100 ng/ml LPS in these conditions (Fig. 6E). In these experiments, cells were preincubated for 30 min with 2 or 5 μM cytochalasin D followed by 4 h of stimulation with 100 ng/ml LPS in the presence of 1 μM cytochalasin D. The reduction of the cytochalasin D concentration during the prolonged LPS action was required due to a toxic effect of higher cytochalasin D doses. After preincubation of cells with 5 μM cytochalasin D followed by 1 μM cytochalasin D, a slight up-regulation of LPS-induced TNF-α-release took place (Fig. 6E).

DISCUSSION

Upon bacterial infection, LPS induces production of numerous pro-inflammatory cytokines and type I interferons by monocytes/macrophages and neutrophils downstream of signaling pathways which have been studied extensively [for review see Lu et al., 2008; McGettrick and O'Neill, 2010]. Yet, the primary response of LPS-stimulated monocytes/macrophages is their migration to the sites of the infection, which in the case of monocytes is initiated by adhesion of the cells to endothelium and extravasation. In this report, we found that 100 ng/ml LPS induced polarization, elongation and ruffling of J774 cells as well as accelerated cell movement in a wound-healing assay. These data are consistent with earlier data on

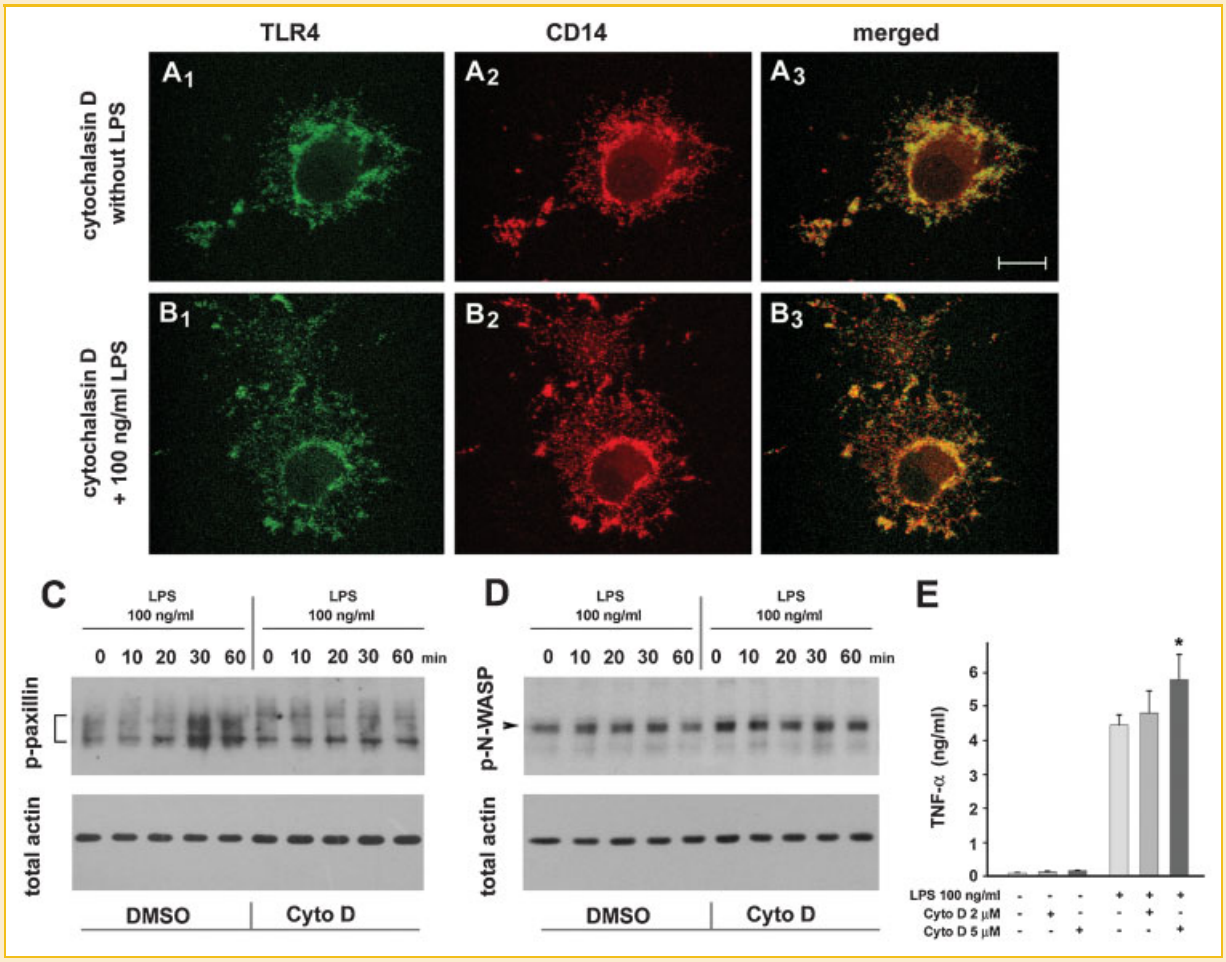

Fig. 6. An influence of cytochalasin D on LPS-triggered signaling. A_1–B_3: Cell surface distribution of TLR4 (A_1,B_1, green), CD14 (A_2,B_2, red) and merged images (A_3,B_3) showing colocalization of the two receptors in the plasma membrane of cytochalasin D-treated cells. Cells were preincubated with 5 μM cytochalasin D or DMSO as a drug carrier and either left unstimulated (upper panel) or exposed to 100 ng/ml LPS for 20 min in the presence of cytochalasin D (lower panel). Bars, 10 μm. C,D: The effect of 5 μM cytochalasin D (Cyto D) on phosphorylation of paxillin on Tyr188 (C) and N-WASP on Ser484/Ser485 (D) in cells. The membranes from the upper panels were reprobed for actin to verify equal loading of proteins on the gels. Data are representative of three experiments. In this set of experiments, phosphorylation of paxillin peaked at 30 min whereas phosphorylation of N-WASP at 20–30 min of stimulation. E: Cytochalasin D slightly up-regulates production of TNF-α induced by 100 ng/ml LPS after 4 h. Data are mean ± SEM from three experiments run in triplicates. *Significantly different from LPS-stimulated cells in the presence of DMSO at $P < 0.05$.

chemokinetic and chemotactic activities of RAW264 cells and Bac1 mouse macrophages stimulated with 1 μg/ml LPS [Williams and Ridley, 2000; Tajima et al., 2008]. LPS-induced activation of cell motility was linked to reorganization of actin cytoskeleton which included polymerization of actin filaments non-soluble in 0.5% Triton X-100 and therefore considered cytoskeletal actin filaments [Hartwig and Shevlin, 1986; Fox et al., 1988]. Their assembly picked after 20 min of LPS action leading to a 1.5-fold increase of the cellular abundance of filamentous actin. An increase of total F-actin level was previously observed in LPS-stimulated RAW264 cells and human neutrophils [Kong and Ge, 2008; Zemans and Arndt, 2009]. Our analysis showed that in the LPS-stimulated cells, cytoskeletal actin filaments polymerized at the expense of actin monomers and the plasma membrane skeleton. The membrane skeleton, comprising about 6% of the total cellular actin in unstimulated cells, underwent substantial depletion under the action of LPS suggesting that the role of this pool of short actin filaments consists in stabilizing the shape of unstimulated cells, as described previously for platelets [Fox et al., 1988]. In resting J774 cells, the plasma membrane skeleton combined with cytoskeletal filaments represented about 40% of cellular actin. This is in reasonable agreement with the F-actin level (about 45%) determined previously by densitometric quantification of actin in 0.75% Triton X-100-insoluble cytoskeleton obtained from lung macrophages [Hartwig and Shevlin, 1986]. These values are lower than F-actin levels in other cells like CHO cells (72.4%) and HeLa cells (57.7%) found by densitometric analysis of 1% Triton X-100-insoluble fraction isolated in the presence of myosin as an F-actin stabilizing agent [Heacock et al., 1984]. Recently, an even higher F-actin proportion (about 75% of total actin) was established in lamellipodia of moving B16-F1 mouse melanoma cells with application of an advanced fluorescence imaging technique [Koestler et al., 2009]. Taken together, the data suggest that unstimulated macrophages contain a relatively low proportion of F-actin in comparison with other cells, although the

effect of different methods for F-actin estimation cannot be ruled out.

We found that the actin polymerization in LPS-stimulated cells correlated with phosphorylation of two actin-regulatory proteins, paxillin, and N-WASP. Paxillin is an adaptor protein involved in multiple protein–protein interactions important for protrusion of the leading edge and formation/disassembly of focal adhesions of moving cells [Petit et al., 2000; Yano et al., 2000; Laukaitis et al., 2001]. Upon challenging of cells with a variety of stimuli, paxillin undergoes phosphorylation on several tyrosine, serine, and threonine residues [Brown and Turner, 2004]. Among those, phosphorylation on Ser126/130 was found crucial for spreading of LPS-stimulated macrophages [Cai et al., 2006]. Paxillin can also be phosphorylated on multiple tyrosine residues including Tyr31, 40, 88, 118, and 181 [Nakamura et al., 2000; Schaller and Schaefer, 2001]. It was found previously that LPS induced bulk tyrosine phosphorylation of paxillin in monocytes and macrophages indicating either a transient or more persistent (30–60 min) character of the process depending on the cell adhesion to the substratum and cell type [Williams and Ridley, 2000; Hazeki et al., 2003]. In our hands, the LPS-induced phosphorylation of paxillin Tyr118 was rapid and transient, picking at 20–30 min of cell stimulation with LPS in correlation with the motile activity of the cells. The phospho-paxillin was revealed in focal adhesions some of which were located at the base of filopodia that are engaged in formation of new focal contacts in moving cells. When phosphorylated, paxillin Tyr118 and Tyr31 create binding sites for the SH2 domain of Crk adaptor proteins which eventually leads to activation of Rac1 GTPase [Schaller and Parsons, 1995; Petit et al., 2000]. Phosphorylation of Tyr118 and Tyr31 in paxillin was found earlier to be required for migration of rat bladder carcinoma NBT-II cells and ephrin B1-stimulated cells owing to the recruitment of Crk [Petit et al., 2000; Vindis et al., 2004] and similar mechanism is likely to control locomotion of LPS-stimulated cells.

Phosphorylation of paxillin is catalyzed by focal adhesion kinase, Abl kinase, and kinases of the Src family [Bellis et al., 1995; Schaller and Schaefer, 2001]. Src kinases have been proposed to control LPS-stimulated phosphorylation of paxillin and spreading of human monocytes [Williams and Ridley, 2000]. In agreement with those results, in our hands, PP2, an inhibitor of Src kinases [Bain et al., 2007], efficiently inhibited the LPS-stimulated phosphorylation of paxillin on Tyr118 and blocked actin polymerization as well. The Src-family kinases important for the LPS-triggered signaling and migration of macrophages are likely to include Src, Lyn, Hck, and Fgr [Lowell and Berton, 1988; Suen et al., 1999; Medvedev et al., 2007; Maa et al., 2008]. An engagement of Src family kinases in LPS-induced activity of actin-regulatory proteins was supported by our data indicating that the kinases indirectly controlled phosphorylation of N-WASP on Ser484/485. Phosphorylation of a closely related protein WASP on Ser483/484 was described by Cory et al. [2003] who also showed that casein kinase 2 can catalyze the reaction in vitro and in vivo. The phosphorylation increases affinity of WASP for the Arp2/3 complex enhancing actin nucleation and polymerization. Only recently, an increased serine phosphorylation of N-WASP has been revealed to accompany migration of insulin-stimulated epithelial cells [Kalwa and Michel, 2011]. We found that LPS moderately increased the N-WASP phosphorylation on Ser484/485 after 20 min of action. The phosphorylated N-WASP was enriched at the leading edge of the LPS-stimulated cells, similarly to the accumulation of $PI(4,5)P_2$, a lipid increasing the actin nucleation activity of N-WASP and WASP [Miki et al., 1996; Higgs and Pollard, 2000; Rohatgi et al., 2000; Tomasevic et al., 2007]. Of note, in the course of cell stimulation with LPS the later dephosphorylation of N-WASP was substantial. The data indicate that phosphorylation of N-WASP can be important for LPS-induced polymerization of actin in macrophages. Dephosphorylation of N-WASP and the resulting decreased affinity for the Arp2/3 complex can provide a mechanism of switching off the polymerization of actin at later stages of LPS action.

The actin-rich leading edge of LPS-stimulated cells was the place where TLR4 and CD14 accumulated and colocalized to a significant degree. On the other hand, disturbances of actin cytoskeleton organization induced by cytochalasin D affected the cell shape and reduced the colocalization rate of the two receptors. Yet, TNF-α production was not inhibited in these conditions. In contrast to our data, Kim et al. [2010] reported that 2.5–20 μM cytochalasin B strongly inhibited TNF-α production in RAW264 cells. Routinely, 20 μM cytochalasin B was used in those studies, therefore, an application of such high doses of cytochalasin B could provide an explanation for its inhibitory actions in RAW264 cells. In our hands, treatment of cells with 5 μM cytochalasin D for 4 h in the presence of 10% DMEM, which reduced its toxic effect, did not inhibit TNF-α production in J774 cells (not shown). These data are in agreement with an earlier report showing that two actin-depolymerizing substances, cytochalasin D, and latranculin B, hardly affected TNF-α production in LPS-stimulated human monocytes [Rossol et al., 2001]. The diverse effects of actin depolymerization on TNF-α production suggest that the role of actin filaments in this process cannot be excluded. On the other hand, LPS-stimulated reorganization of the actin cytoskeleton leading to cell polarization and concomitant translocation of TLR4 and CD14 to the front of cells are not required for efficient production of TNF-α. Of note, the aforementioned Hck/Fgr-deficient mice showed a high level of serum TNF-α despite the fact that neutrophils of those mice revealed reduced migration into tissues [Lowell and Berton, 1988]. Altogether, the data suggest that LPS-stimulated migration of cells is not a prerequisite for TNF-α release.

ACKNOWLEDGMENTS

We thank Kazimiera Mrozinska for excellent technical assistance. This work was supported by grant N N301 555240 from the National Science Center to K.K. and by fellowships from Jozef Mianowski Found to G.K. and M.Z.

REFERENCES

Bain J, Plater L, Elliott M, Shpiro N, Hastie CJ, McLauchlan H, Klevernic I, Arthur JS, Alessi DR, Cohen P. 2007. The selectivity of protein kinase inhibitors: A further update. Biochem J 408:297–315.

Bellis SL, Miller JT, Turner CE. 1995. Characterization of tyrosine phosphorylation of paxillin in vitro by focal adhesion kinase. J Biol Chem 270:17437–17441.

Brown MC, Turner CE. 2004. Paxillin: Adapting to change. Physiol Rev 84: 1315–1339.

Cai X, Li M, Vrana J, Schaller MD. 2006. Glycogen synthase kinase 3- and extracellular signal-regulated kinase-dependent phosphorylation of paxillin regulates cytoskeletal rearrangement. Mol Cell Biol 26:2857–2868.

Continolo S, Baruzzi A, Majeed M, Caveggion E, Fumagalli L, Lowell CA, Berton G. 2005. The proto-oncogene Fgr regulates cell migration and this requires its plasma membrane localization. Exp Cell Res 302:253–269.

Cory GO, Cramer R, Blanchoin L, Ridley AJ. 2003. Phosphorylation of the WASP-VCA domain increases its affinity for the Arp2/3 complex and enhances actin polymerization by WASP. Mol Cell 11:1229–1239.

Fox JE, Boyles JK, Berndt MC, Steffen PK, Anderson LK. 1988. Identification of a membrane skeleton in platelets. J Cell Biol 106:1525–1538.

Fumagalli L, Zhang H, Baruzzi A, Lowell CA, Berton G. 2007. The Src family kinases Hck and Fgr regulate neutrophil responses to *N*-formyl-methionyl-leucyl-phenylalanine. J Immunol 178:3874–3885.

Hartwig JH, Shevlin P. 1986. The architecture of actin filaments and the ultrastructural location of actin-binding protein in the periphery of lung macrophages. J Cell Biol 103:1007–1020.

Hazeki K, Masuda N, Funami K, Sukenobu N, Matsumoto M, Akira S, Takeda K, Seya T, Hazeki O. 2003. Toll-like receptor-mediated tyrosine phosphorylation of paxillin via MyD88-dependent and -independent pathways. Eur J Immunol 33:740–747.

Heacock CS, Eidsvoog KE, Bamburg JR. 1984. The influence of contact-inhibited growth and of agents which alter cell morphology on the levels of G- and F-actin in cultured cells. Exp Cell Res 153:402–412.

Higgs HN, Pollard TD. 2000. Activation by Cdc42 and PIP_2 of Wiskott–Aldrich syndrome protein (WASp) stimulates actin nucleation by Arp2/3 complex. J Cell Biol 150:1311–1320.

Kagan JC, Medzhitov R. 2006. Phosphoinositide-mediated adaptor recruitment controls Toll-like receptor signaling. Cell 125:943–955.

Kagan JC, Su T, Horng T, Chow A, Akira S, Medzhitov R. 2008. TRAM couples endocytosis of Toll-like receptor 4 to the induction of interferon-β. Nat Immunol 9:361–368.

Kalwa H, Michel T. 2011. The MARCKS protein plays a critical role in PIP_2 metabolism and directed cell movement in vascular epithelial cell. J Biol Chem 286:2320–2330.

Kawai T, Takeuchi O, Fujita T, Inoue J, Mühlradt PF, Sato S, Hoshino K, Akira S. 2001. Lipopolysaccharide stimulates the MyD88-independent pathway and results in activation of IFN-regulatory factor 3 and the expression of a subset of lipopolysaccharide-inducible genes. J Immunol 167:5887–5894.

Kim JY, Lee YG, Kim MY, Byeon SE, Rhee MH, Park J, Katz DR, Chain BM, Cho JY. 2010. Src-mediated regulation of inflammatory responses by actin polymerization. Biochem Pharmacol 79:431–443.

Koestler SA, Rottner K, Lai F, Block J, Vinzenz M, Small JV. 2009. F- and G-actin concentrations in lamellipodia of moving cells. PLoS ONE 4:e4810.

Kong L, Ge BX. 2008. MyD88-independent activation of a novel actin-Cdc42/Rac pathway is required for Toll-like receptor-stimulated phagocytosis. Cell Res 18:745–755.

Kulma M, Herec M, Grudzinski W, Anderluh G, Gruszecki WI, Kwiatkowska K, Sobota A. 2010. Sphingomyelin-rich domains are sites of lysenin oligomerization: Implications for raft studies. Biochim Biophys Acta 1798:471–481.

Kwiatkowska K, Frey J, Sobota A. 2003. Phosphorylation of FcγRIIA is required for the receptor-induced actin rearrangement and capping: The role of membrane rafts. J Cell Sci 116:537–550.

Laukaitis CM, Webb DJ, Donais K, Horwitz AF. 2001. Differential dynamics of α5 integrin, paxillin, and alpha-actinin during formation and disassembly of adhesions in migrating cells. J Cell Biol 153:1427–1440.

Lowell CA, Berton G. 1988. Resistance to endotoxic shock and reduced neutrophil migration in mice deficient for the Src-family kinases Hck and Fgr. Proc Natl Acad Sci USA 95:7580–7584.

Lu YC, Yeh WC, Ohashi PS. 2008. LPS/TLR4 signal transduction pathway. Cytokine 42:145–151.

Maa MC, Chang MY, Chen YJ, Lin CH, Yu CJ, Yang YL, Li J, Chen PR, Tang CH, Lei HY, Leu TH. 2008. Requirement of inducible nitric-oxide synthase in lipopolysaccharide-mediated Src induction and macrophage migration. J Biol Chem 283:31408–31416.

Machesky LM, Insall RH. 1998. Scar1 and the related Wiskott–Aldrich syndrome protein WASP, regulate the actin cytoskeleton through the Arp2/3 complex. Curr Biol 8:1347–1356.

Manders EMM, Verbkeed FJ, Aten JA. 1993. Measurements of co-localization of objects in dual-color confocal images. J Microsc 169:375–382.

McGettrick AF, O'Neill LA. 2010. Regulators of TLR4 signaling by endotoxins. Subcell Biochem 53:153–171.

Medvedev AE, Piao W, Shoenfelt J, Rhee SH, Chen H, Basu S, Wahl LM, Fenton MJ, Vogel S. 2007. Role of TLR4 tyrosine phosphorylation in signal transduction and endotoxin tolerance. J Biol Chem 282:16042–16453.

Miki H, Miura K, Takenawa T. 1996. N-WASP, a novel actin-depolymerizing protein, regulates the cortical cytoskeletal rearrangement in a PIP2-dependent manner downstream of tyrosine kinases. EMBO J 15:5326–5335.

Nakagawa H, Miki H, Ito M, Ohashi K, Takenawa T, Miyamoto S. 2001. N-WASP, WAVE and Mena play different roles in the organization of actin cytoskeleton in lamellipodia. J Cell Sci 114:1555–1565.

Nakamura K, Yano H, Uchida H, Hashimoto S, Schaefer E, Sabe H. 2000. Tyrosine phosphorylation of paxillin α is involved in temporospatial regulation of paxillin-containing focal adhesion formation and F-actin organization in motile cells. J Biol Chem 275:27155–27164.

Park BS, Song DH, Kim HM, Choi BS, Lee H, Lee JO. 2009. The structural basis of lipopolysaccharide recognition by the TLR4-MD-2 complex. Nature 458: 1191–1195.

Petit V, Boyer B, Lentz D, Turner CE, Thiery JP, Valles AM. 2000. Phosphorylation of tyrosine residues 31 and 118 on paxillin regulates cell migration through an association with CRK in NBT-II cells. J Cell Biol 148:957–970.

Pollard TD, Borisy GG. 2003. Cellular motility driven by assembly and disassembly of actin filaments. Cell 112:453–465.

Poltorak A, He X, Smirnova I, Liu MY, Van Huffel C, Du X, Birdwell D, Alejos E, Silva M, Galanos C, Freudenberg M, Ricciardi-Castagnoli P, Layton B, Beutler B. 1998. Defective LPS signaling in C3H/HeJ and C57BL/10ScCr mice: Mutations in Tlr4 gene. Science 282:2085–2088.

Rohatgi R, Ho HY, Kirschner MW. 2000. Mechanism of N-WASP activation by CDC42 and phosphatidylinositol 4,5-bisphosphate. J Cell Biol 150:1299–1310.

Rossol M, Gartner D, Hauschildt S. 2001. Diverse regulation of microfilament assembly, production of TNF-α, and reactive oxygen intermediates by actib modulating substance and inhibitors of ADP-ribosylation in human monocytes stimulated with LPS. Cell Motil Cytoskeleton 48:96–108.

Schaller MD, Parsons JT. 1995. pp125FAK-dependent tyrosine phosphorylation of paxillin creates a high-affinity binding site for Crk. Mol Cell Biol 15:2635–2645.

Schaller MD, Schaefer EM. 2001. Multiple stimuli induce tyrosine phosphorylation of the Crk-binding sites of paxillin. Biochem J 360:57–66.

Suen PW, Ilic D, Caveggion E, Berton G, Damsky CH, Lowell CA. 1999. Impaired integrin-mediated signal transduction, altered cytoskeletal structure and reduced motility in Hck/Fgr deficient macrophages. J Cell Sci 112: 4067–4078.

Szymanska E, Korzeniowski M, Raynal P, Sobota A, Kwiatkowska K. 2009. Contribution of PIP-5 kinase Iα to raft-based FcγRIIA signaling. Exp Cell Res 315:981–995.

Tajima T, Murata T, Aritake K, Urade Y, Hirai H, Nakamura M, Ozaki H, Hori M. 2008. Lipopolysaccharide induces macrophage migration via prostaglandin D_2 and prostaglandin E_2. J Pharmacol Exp Ther 326:493–501.

Tomasevic N, Jia Z, Russell A, Fujii T, Hartman JJ, Clancy S, Wang M, Berdau C, Wood KW, Sakowicz R. 2007. Differential regulation of WASP and N-WASP by Cdc42, Rac1, Nck, and PI(4,5)P_2. Biochemistry 46:3494–3502.

Vindis C, Teli T, Cerretti DP, Turner CE, Huynh-Do U. 2004. EphB1-mediated cell migration requires the phosphorylation of paxillin at Tyr-31/Tyr-118. J Biol Chem 279:27965–27970.

Weintz G, Olsen JV, Fruhauf K, Niedzielska M, Amit I, Jantsch J, Mages J, Frech C, Dolken L, Mann M, Lang R. 2010. The phosphoproteome of toll-like receptor-activated macrophages. Mol Syst Biol 6:371.

Williams LM, Ridley AJ. 2000. Lipopolysaccharide induces actin reorganization and tyrosine phosphorylation of Pyk2 and paxillin in monocytes and macrophages. J Immunol 164:2028–2036.

Wu X, Suetsugu S, Cooper LA, Takenawa T, Guan J-L. 2004. Focal adhesion kinase regulation of N-WASP subcellular localization and function. J Biol Chem 279:9565–9576.

Yano H, Uchida H, Iwasaki T, Mukai M, Akedo H, Nakamura K, Hashimoto S, Sabe H. 2000. Paxillin α and Crk-associated substrate exert opposing effects on cell migration and contact inhibition of growth through tyrosine phosphorylation. Proc Natl Acad Sci USA 97:9076–9081.

Zemans RL, Arndt PG. 2009. Tec kinases regulate actin assembly and cytokine expression in LPS-stimulated human neutrophils via JNK activation. Cell Immunol 258:90–97.